Ab initio reflectance difference spectra of the bare and adsorbate covered Cu(110) surfaces

J. Harl and G. Kresse*
Faculty of Physics, Universität Wien and Center for Computational Materials Science, Sensengasse 8, A-1090 Wien, Austria

L. D. Sun, M. Hohage, and P. Zeppenfeld
Institute of Experimental Physics, Atomic Physics and Surface Science, Johannes Kepler University Linz, Altenbergerstrasse 69, A-4040 Linz, Austria

(Received 21 December 2006; revised manuscript received 23 April 2007; published 27 July 2007)

The reflectance difference spectra of the bare Cu(110) surface, of the oxygen induced (2×1)O reconstruction, and of the carbon monoxide covered Cu(110) surface are calculated using density functional theory and the independent particle approximation. Generally, good agreement with experiment is found at energies below 2 eV, where a resonance between two surface states dominates the spectrum for the bare surface. The resonance is progressively quenched from the bare surface, over the oxygen covered surface, to the CO covered surface. At higher energies, a rather deep minimum in the reflectance difference spectrum is calculated for all three surfaces, which agrees qualitatively with experiment, but details such as the shape and depth of the minimum are not in good agreement with experiment. We argue that a treatment beyond standard density functional theory is required at higher energies, in particular, for adsorbate covered surfaces. The calculated spectra and the surface band structures are carefully analyzed with respect to transitions between specific electronic states, confirming previous experimental and theoretical assignments. An essential result of the study is that the anisotropy of the intraband plasma frequency tensor (Drude-like term) is important and must be calculated on the same level of theory as the interband contributions to the dielectric function. Only then the results converge with increasing layer numbers.

DOI: 10.1103/PhysRevB.76.035436 PACS number(s): 78.40.−q, 78.68.+m, 73.20.−r, 68.43.Bc

I. INTRODUCTION

Reflectance difference (RD) spectroscopy has proven to be a powerful technique to probe anisotropic metallic surfaces.[1] A complete interpretation of the RD spectrum, nevertheless, cannot be given without a detailed knowledge of the surface dielectric function and its anisotropy.

RD spectroscopy measures the difference of the reflectivity of normal incident light, which is linearly polarized along two perpendicular directions (x and y), parallel to the surface plane.[2] The relationship between the measured signal $\Delta r/\bar{r} = 2(r_x - r_y)/(r_x + r_y)$ and the anisotropy of the dielectric function $\Delta\varepsilon^s = \varepsilon_x^s - \varepsilon_y^s$ is given in the thin film limit of the model of Aspnes and co-workers[3–5] of Aspnes and co-workers by

$$\frac{\Delta r}{\bar{r}} = -\frac{2i\omega d}{c}\left[\frac{\Delta\varepsilon^s(\omega)}{\varepsilon^b(\omega)-1}\right]. \quad (1)$$

Thus, in principle, the reflectance difference can be approximated by the ratio of the difference of the (complex) surface dielectric function $\Delta\varepsilon^s$ and the bulk dielectric function ε^b, weighted with the frequency ω of the incident light and divided by the velocity of light c. The thickness of the surface region d enters linearly as long as d is much smaller than the wavelength λ of the incident light.

The quantity accessible to *ab initio* density functional theory calculations is the dielectric function, which, in the present work, is evaluated in the independent particle picture.[6,7] As the momentum transfer of visible light is small compared to the Brillouin zone size, only the long wavelength limit is considered. We have performed test calculations which show that, at least for the bulk, local field effects can be neglected.

Optical calculations on metallic bulk systems are numerous, ranging from calculations of the dielectric function and loss functions in the long wavelength limit (e.g., Ref. 8), over investigations of the dynamical response function,[9,10] to a variety of studies on magneto-optical properties (e.g., Refs. 11–13). Density functional theory (DFT) calculations on the reflectance difference of metallic surfaces are fairly scarce because of the large computational cost required for evaluating the optical response of the surface. Theoretical RD spectra available so far have been calculated for the bare Cu(110) and Ag(110) surfaces and for the carbon monoxide covered Cu(110) surface.[14–16] Additionally, the reflectance difference spectrum of the Al(110) surface has been investigated.[17]

Although the reflectance spectra for the bare and CO covered Cu(110) surfaces calculated by Monachesi *et al.* showed no perfect resemblance to the experimental spectra, the main features were reproduced. Furthermore, the spectrum of the bare Cu(110) surface[14,15] was analyzed in terms of contributions from and to surface or bulklike states. The belief expressed in many experimental studies (starting with Ref. 18) that the strong reflectance anisotropy of the Cu(110) surface at 2 eV is due to a transition between two surface states was confirmed in Ref. 14.

Obviously, an interpretation of the Cu(110) RD spectrum just considering RD features related to the dielectric function of the bulk (a summary of bulk related effects is given in Ref. 19) is not possible, and an *ab initio* calculation of the anisotropic dielectric function based on the surface band structure is required.

In the present work, we calculate the reflectance difference spectra of the bare Cu(110) surface, the oxygen induced (2×1)O reconstruction, and the CO covered surface, all of which have been extensively studied experimentally.[18,20–25]

The surfaces are modeled by slabs with up to 25 layers, in contrast to 11 layers used in the work of Monachesi *et al.*[14–16] We especially focus on the layer convergence of the RD spectra, which is found to be a critical point of the theoretical approach, and address the importance of including the anisotropic surface plasma frequency calculated *ab initio*. The observed RD features are assigned to excitations arising from specific areas of the Brillouin zone and one particle energy regions, offering the possibility to relate specific features of the RD spectrum to transitions between particular bands.

II. THEORY

A. Dielectric function

The imaginary part of the interband dielectric tensor $\varepsilon_{\alpha\beta}^{2,\mathrm{inter}}$ was calculated within the independent particle picture. Local field effects were neglected and the long wavelength limit was considered. For a periodic system described by a unit cell with volume Ω, the imaginary part of the interband dielectric tensor with respect to the Cartesian directions e_α and e_β is given by (here and in the following, we use cgs units)

$$\varepsilon_{\alpha\beta}^{2,\mathrm{inter}}(\omega) = \frac{4\pi^2 e^2}{\Omega} \lim_{q\to 0} \frac{1}{q^2} \sum_{n\neq m;\mathbf{k}} 2 f_{n\mathbf{k}} g_{\mathbf{k}} \langle u_{m\mathbf{k}+q\mathbf{e}_\alpha} | u_{n\mathbf{k}} \rangle \times \langle u_{m\mathbf{k}+q\mathbf{e}_\beta} | u_{n\mathbf{k}} \rangle^* [\delta(\epsilon_{m\mathbf{k}} - \epsilon_{n\mathbf{k}} - \hbar\omega) - \delta(\epsilon_{m\mathbf{k}} - \epsilon_{n\mathbf{k}} + \hbar\omega)]. \quad (2)$$

The cell periodic part of the Bloch functions for band n and k-point $\mathbf{k}$ is denoted as $u_{n\mathbf{k}}$. The momentum transfer from the incident light with wave vector q is small compared to the Brillouin zone size. The occupation number of the DFT one-electron orbital $u_{n\mathbf{k}}$ with energy $\epsilon_{n\mathbf{k}}$ is given by $f_{n\mathbf{k}}=f(\epsilon_{n\mathbf{k}})$. The weighting factors $g_{\mathbf{k}}$ account for the fact that the summation is only performed over the irreducible part of the Brillouin zone and they sum to 1. A detailed description of the evaluation of this expression in the Vienna *Ab Initio* Simulation package (VASP) is given in Ref. 26.

The imaginary part of the intraband term $\varepsilon_{\alpha\beta}^{2,\mathrm{intra}}$ can be explicitly described by just considering transitions between the same band and expanding terms with respect to the photon wave vector $\mathbf{q}$ (see, e.g., Ref. 27). Without considering damping, the imaginary part of the intraband dielectric function vanishes for all frequencies other than zero. The real part of the dielectric function is related to the imaginary part via the Kramers-Kronig relation:

$$\varepsilon_{\alpha\beta}^{1}(\omega) = \left[1 + \frac{1}{\pi}\mathbf{P}\int \frac{\varepsilon_{\alpha\beta}^{2,\mathrm{intra}}(\omega')}{\omega'-\omega} d\omega'\right] + \frac{1}{\pi}\mathbf{P}\int \frac{\varepsilon_{\alpha\beta}^{2,\mathrm{inter}}(\omega')}{\omega'-\omega} d\omega' =: \varepsilon_{\alpha\beta}^{1,\mathrm{intra}}(\omega) + \varepsilon_{\alpha\beta}^{1,\mathrm{inter}}(\omega), \quad (3)$$

with $\mathbf{P}$ being the principal value of the integrals. The real part of the intraband dielectric function $\varepsilon_{\alpha\beta}^{1,\mathrm{intra}}$ can be expressed as

$$\varepsilon_{\alpha\beta}^{1,\mathrm{intra}}(\omega) = 1 - \frac{\bar{w}_{\alpha\beta}^2}{\omega^2}, \quad (4)$$

with the square of the intraband plasma frequency tensor $\bar{w}_{\alpha\beta}$ given by (see, e.g., Ref. 27)

$$\bar{w}_{\alpha\beta}^2 = \frac{4\pi e^2}{\Omega\hbar^2} \sum_{n,\mathbf{k}} 2 g_{\mathbf{k}} f_{n\mathbf{k}} \left(\mathbf{e}_\alpha \frac{\partial}{\partial \mathbf{k}}\right)\left(\mathbf{e}_\beta \frac{\partial}{\partial \mathbf{k}}\right) \epsilon_{n\mathbf{k}}. \quad (5)$$

This can be rewritten as (discretized) integral over the Fermi surface[9]

$$\bar{w}_{\alpha\beta}^2 = \frac{4\pi e^2}{\Omega\hbar^2} \sum_{n,\mathbf{k}} 2 g_{\mathbf{k}} \frac{\partial f(\epsilon_{n\mathbf{k}})}{\partial \epsilon} \left(\mathbf{e}_\alpha \frac{\partial \epsilon_{n\mathbf{k}}}{\partial \mathbf{k}}\right)\left(\mathbf{e}_\beta \frac{\partial \epsilon_{n\mathbf{k}}}{\partial \mathbf{k}}\right). \quad (6)$$

In the present work, the plasma frequency tensor $\bar{w}_{\alpha\beta}$ has been calculated using Eq. (6) for all considered systems. As shown below, the anisotropy of the tensor $\bar{w}_{\alpha\beta}$ is essential for an accurate determination of the RD spectra.

B. Technical details

The present density functional theory calculations have been performed using VASP.[28,29] Within this plane wave basis set code, the interaction between the ionic cores and the valence electrons is described by the projector-augmented wave (PAW) method[30] in the implementation of Kresse and Joubert.[31] Generalized gradient approximations of Perdew, Burke, and Ernzerhof,[32] commonly referred to as PBE, are used throughout this work to represent the exchange-correlation energy. A description of the actual implementation of the optical routines within the PAW formalism is given in Ref. 26.

The bare Cu(110), the Cu(110)-(2×1)O, and the Cu(110)-$(n\times1)$CO $(n=2,3)$ surfaces were represented by repeated slabs constructed of 12–25 copper layers and a vacuum region of 10 Å (corresponding to approximately eight layers). The adsorbates were placed on both sides of the slab. The (1×1) unit cell of the bare Cu(110) surface is spanned by two orthogonal vectors with lengths $a/\sqrt{2}$ in the $[1\bar{1}0]$ direction and a in the $[001]$ direction. In the following, we will refer to the $[1\bar{1}0]$, $[001]$, and $[110]$ directions also as the x, y, and z directions, respectively. For the lattice constant a, we have chosen the PBE value of 3.638 Å, which is slightly larger than the experimental lattice constant of 3.615 Å. The surface cells of the (2×1)O and the (2×1)CO surfaces are twice as large in the $[1\bar{1}0]$ direction.

The (2×1)O reconstruction is characterized by Cu-O-Cu rows along the $[001]$ direction, with oxygen atoms placed in short bridge sites and additional Cu atoms in hollow sites. Illustrations and *ab initio* calculations of the geometric parameters using the same DFT code have been presented previously by Liem *et al.*[33] and Harl and Kresse.[34]

Experimentally, CO is found to adsorb on the top site with a C-Cu distance of 1.87 Å and a C-O bond length of 1.11 Å (see, e.g., Hofmann *et al.*[35]). As for the bare and the (2×1)O surface, we relaxed the outermost three Cu layers and the adsorbates prior to all optical calculations. The (2×1)CO surface relaxation yields a C-Cu distance of

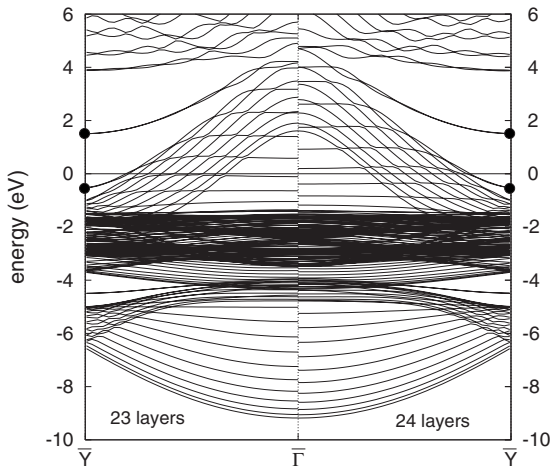

FIG. 1. Energy bands of the bare Cu(110) surface between the $\bar{\Gamma}$ and $\bar{Y}$ points for 23 and 24 layers. The energies are given with respect to the Fermi energy. Surface bands are indicated by filled circles at the $\bar{Y}$ point.

1.84 Å and a C-O distance of 1.16 Å, which are both within a few percent of the experimental values.

The calculations of the RD spectra presented in this work were carried out using Eq. (2) to determine the dielectric function in the $[1\bar{1}0]$ and [001] directions. The Drude-like term, as defined in Eq. (4), with the anisotropic intraband plasma frequency tensor [Eq. (6)], was included in the dielectric function. The thickness d in Eq. (1) is given by the height of the supercell normal to the surface plane, so that the surface dielectric function becomes an intrinsic function of the surface area.

The convergence of the surface dielectric function with respect to the number of k points is slow, because the magnitude of a transition depends strongly on the k-point position, and a coarse sampling of the Brillouin zone, therefore, neglects important contributions to the dielectric function. Tests for the k-point density show that using a $(40\times24\times1)$ k-point set for the bare Cu(110) surface, a $(20\times24\times1)$ k-point set for the (2×1) periodic surfaces, and a $(12\times24\times1)$ k-point set for the (3×1) surface, the dielectric functions are well described. For the integration over the Brillouin zone, we used the first order Methfessel-Paxton method[36] with a width of 0.2 eV. This width is low enough to conserve the main features of the dielectric function and, at the same time, large enough to allow convergence of the intraband plasma frequency tensor. The thickness dependence of the RD spectra, a critical point when simulating a macroscopic surface by a slab of a few atomic layers, is addressed in the following paragraph.

Figure 1 shows the energy bands along the $\bar{\Gamma}$-$\bar{Y}$ direction for a bare Cu(110) slab with 23 and 24 layers. Obviously, the position of the surface bands (at approximately −0.5 eV and 1.5 eV) at the $\bar{Y}$ point is the same for 23 and 24 layers. Even for 12 layers, the surface band positions are well converged. On the other hand, bulklike bands are situated at different positions for different slab thicknesses. This implies slower convergence for transitions involving bulklike bands.

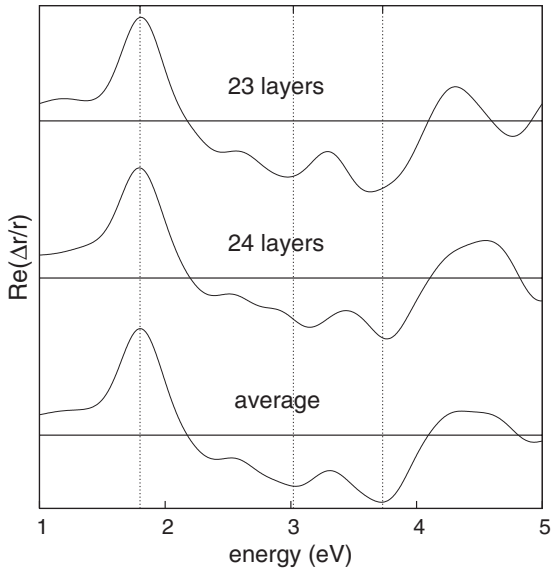

FIG. 2. Reflectance difference spectrum for 23 and 24 layers (two upper panels) and the averaged RD spectrum obtained by averaging the results for 23, 24, and 25 layers as discussed in the text.

In order to examine the effect introduced by the finite thickness of the slab, the optical properties of the four Cu surfaces were calculated for 23, 24, and 25 layer Cu slabs. Due to the finite size of the slab, the discretized band structure introduces artifacts that lead to slightly different spurious oscillations in the dielectric functions and RD spectra for 23, 24, and 25 layers, respectively. In order to minimize this discretization effect, the final RD spectra were determined by averaging first over 23 and 24 layers, then 24 and 25 layers, and finally, averaging over these two results. The justification for this procedure is illustrated by a comparison of the band structure of the 23 and 24 layer slabs (see Fig. 1). In the case of Cu(110), the onset positions of the *sp* bulklike bands are roughly alternating for slabs with one layer difference. Transitions between localized bands (*d* bands) and *sp*-like bands, therefore, show alternating onsets for slabs with one layer difference. These artifacts, arising from the coarse spacing of the bulklike bands, can be reduced by averaging. Figure 2 reveals the thickness dependency of the RD spectrum for the bare surface. The upper two panels show the RD spectra for 23 and 24 layers; the third RD spectrum is the result of the average over 23, 24, and 25 layers. Positions of distinct features in the RD spectrum are indicated by the dotted lines. Obviously, the fine structure of the RD spectra varies with the thickness of the slab. The main features, nevertheless, remain qualitatively the same for all slabs.

For the interpretation of the RD spectra and identification of the origin of the main RD spectrum (RDS) features, the contributions to the dielectric function have been separated according to their k vector and energy origin.

III. RESULTS

A. Interband contributions at low energies

For semiconductors and insulators, a threshold energy for optical transitions exists, which is given by the band gap of

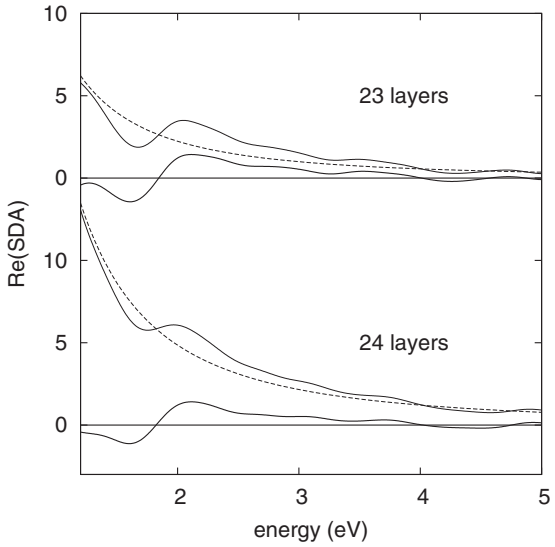

FIG. 3. Real part of the surface dielectric anisotropy (SDA) for the 23 and 24 layer Cu(110) slabs. The thin line shows the SDA considering only interband contributions. The SDA arising from the anisotropic intraband term, whose magnitude is given by the intraband plasma frequency, is the negative of the curve shown with a dashed line. The SDA considering both interband and intraband contributions is plotted with a thick line.

the material. For metals, interband transitions between bands with vanishing energy differences cannot be excluded. Brust[37] and Szmulowicz and Segall[38] were the first to suggest such interband contributions. They arise from transitions between bands crossing near the Fermi edge and are, therefore, accessible for excitations activated by photons with low energies (where "low energies" in the present context refers to energies smaller than 1 eV). For metallic surfaces, these contributions can become huge because of the repeated crossing of bulklike bands near the Fermi energy (see Fig. 1). The magnitude of the low energy interband contributions to the imaginary part of the dielectric function is, on one hand, anisotropic with respect to the surface direction and, on the other hand, sensitive to the positions of the crossings, which themselves depend on the thickness of the slab. In the energy range considered in this work for the calculation of the RD spectra (1.0–5.0 eV), these low energy transitions show influence via the real part of the dielectric function, which exhibits a $-\beta/\omega^2$ decay, with β depending on the intensity of the low energy transitions. This dependence can be proven by expanding the real part of the interband dielectric function, assuming the transition energies to be much smaller than the considered frequency.

The effect introduced by low frequency interband transitions is illustrated in Fig. 3 for the 23 and 24 layer bare Cu(110) slabs. The difference of the real part of the interband dielectric function in the $[1\bar{1}0]$ and [001] directions (x and y directions, respectively), i.e., the real part of the surface dielectric anisotropy $\mathrm{Re}(\varepsilon_x^s - \varepsilon_y^s)$ [Re(SDA)], is shown as a thin solid line. The low frequency transition probabilities are larger for the [001] direction than for the $[1\bar{1}0]$ direction, causing a stronger $-1/\omega^2$ decay for the real part of the dielectric function along the [001] direction and, consequently, larger positive values at low frequencies for Re(SDA). It is obvious that the interband part alone behaves qualitatively different at small energies for 23 and 24 layers.

This bothersome behavior can be remedied by calculating not only the interband dielectric function but also the intraband dielectric function *ab initio* [Eq. (6)]. The squared intraband plasma frequency, as, e.g., shown in Ref. 37, is given by the total electron density minus the sum over all transition probabilities between two different states divided by their energy difference. Therefore, the plasma frequency is smaller the larger the constant β is in the real part of the interband contributions to the dielectric function. As a consequence, pronounced transitions at low energies will result in a smaller intraband plasma frequency. Thus, for the 23 and 24 layer Cu(110) slab, the intraband plasma frequency is smaller for the [001] direction than for the $[1\bar{1}0]$ direction (6.7 vs 7.1 eV for 23 layers, and 6.3 vs 7.2 eV for 24 layers). The error introduced by neglecting the anisotropic intraband term (shown by dashed lines in Fig. 3) can be appreciated by comparing the thin lines in Fig. 3, where only the interband contributions are considered, to the thick lines, where both interband and intraband transitions are included. If both interband and intraband contributions are correctly accounted for (thick line), the results for the 23 and 24 layer slabs become very similar.

We finally note that for bulk copper the plasma frequency calculated from Eq. (6) is found to be 8.93 eV. Experiments by Johnson and Christy[39] yield an optical mass of $1.49m_e$. For the experimental Cu lattice constant of 3.615 Å, this optical mass corresponds to a plasma frequency of 8.9 eV, which is in excellent agreement with our theoretical value.

B. Band structure of bare Cu(110), Cu(110)-(2×1)O, and Cu(110)-(2×1)CO

For a better understanding of the RD spectra, a detailed knowledge of the band structure is essential. On one hand, the surface band structure will allow us to relate RDS features to specific areas of the Brillouin zone and to specific regions of energy. On the other hand, discrepancies between the DFT energies and the experimental band structure will result in energy shifts between the calculated and measured RD spectra, which have to be kept in mind when comparing DFT and experimental spectra. Although DFT has been shown to reproduce the main features of the band structures, it is known that absolute band energies are less well reproduced. A comparison of the DFT, the GW, and the experimental band structure of bulk Cu can be found in Ref. 40.

Figure 4 shows the calculated band structure of the bare surface represented by a 24 layer slab. The occupied (p_y like) and unoccupied (s like) surface states at the $\bar{Y}$ point are clearly visible. The occupied surface band is located at an energy of −0.5 eV [experiment: −0.4 eV (Ref. 41)] and the unoccupied surface state at 1.5 eV [experiment 1.8 eV (Ref. 42)]. The surface states at the $\bar{X}$ point are both unoccupied at energies of 1.7 and 5 eV. Experiments suggest slightly higher energies of 2.2 and 5.5 eV.[43] The width of the d band is larger than in experiments. Whereas angle-resolved

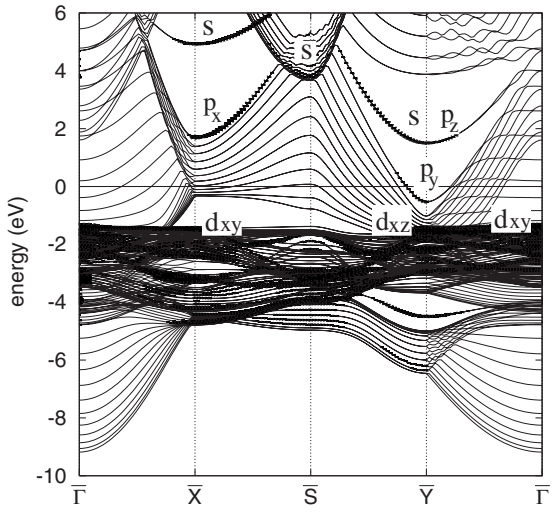

FIG. 4. Band structure of the bare 24 layer Cu(110) slab with important contributions marked by small squares. For explanation of the states, see the text.

ultraviolet photoemission spectroscopy measurements[44] reveal *d* bands between −4.0 and −2.0 eV, the *d* bands still can be found at energies up to −1.5 eV in the DFT calculations. This also holds for the Cu(110)-(2×1)O and Cu(110)-(2×1)CO band structures shown in Fig. 5. Because of the doubled lattice constant in the $[1\bar{1}0]$ direction, the Cu bands are folded back in the *x* direction.

The dominant features of the (2×1)O reconstruction (see top of Fig. 5) are the bands arising from the strong bonds between the oxygen and copper atoms, which form the added rows along the [001] direction. The band with the strongest dispersion along the Cu-O-Cu rows has predominantly O p_y character. Along $\bar{S}'$-$\bar{Y}$, this O p_y orbital hybridizes with Cu orbitals with *s*-like symmetry, Cu $d_{x^2-y^2}$ and Cu d_{z^2}, leading to a strong bonding linear combination located at −7.8 eV below the Fermi level. The respective antibonding linear combinations with O p_y, Cu $d_{x^2-y^2}$, Cu d_{z^2}, and Cu p_z character are visible as weak resonances 0.5 eV above the Fermi level. Along $\bar{\Gamma}$-$\bar{X}'$, the O p_y derived band is located at lower absolute binding energies (−5.2 eV). Due to symmetry, bonding linear combinations can be formed only with the less favorable Cu p_y orbital.

The O p_x and O p_z orbitals show weaker dispersion. Along $\bar{S}'$-$\bar{Y}$, the localization is most pronounced. The O p_z orbital is located somewhat below the O p_x one (−6.0 and −5.5 eV at the $\bar{Y}$ point, respectively). The O p_x orbital hybridizes with the Cu d_{xy} orbital, whereas the O p_z orbital interacts with the Cu d_{yz} state. Also, the antibonding linear combinations are clearly discernible in the band structure (−0.7 and −1.0 eV at the $\bar{Y}$ point). Experimentally,[44] the bonding O *p* bands at the $\bar{Y}$ point have been associated with signals at −7.8, −6.5, and −6.1 eV for the O p_y, the O p_z, and the O p_x bands, respectively. An antibonding resonance at −1.2 eV has been identified as a p_x type orbital. At −1.4 eV, a peak of either p_y or p_z character has been detected. Our calculations suggest that this occupied band is of p_z type, and

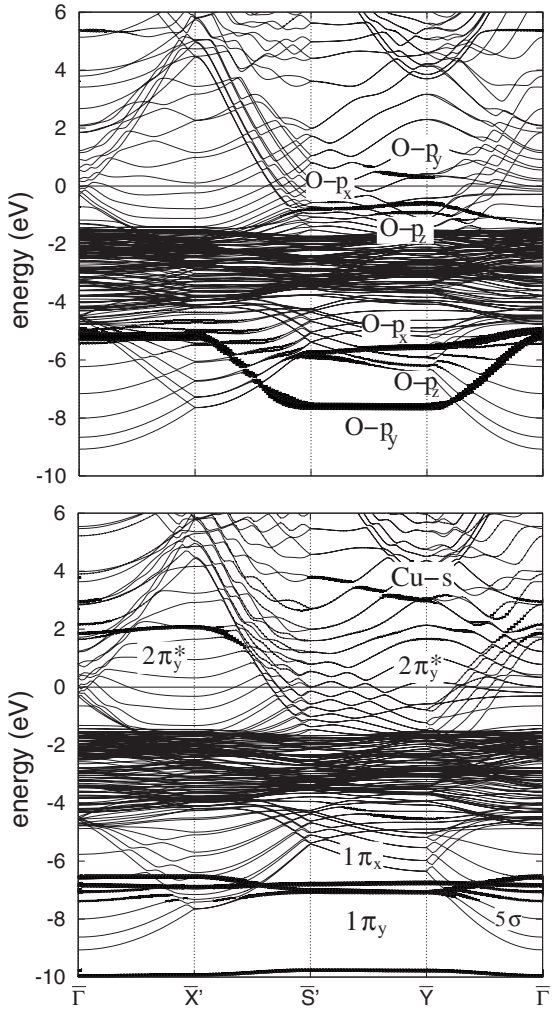

FIG. 5. Band structure of the (2×1)O and (2×1)CO surfaces (12 layer slab). Because of the doubled cell size in the $[1\bar{1}0]$ direction, the Brillouin zone is folded back with respect to the Brillouin zone of the bare surface, and the number of bands is doubled.

that the p_y antibonding state lies above the Fermi energy.

The band structure of the Cu(110)-(2×1)CO surface is shown in the bottom panel of Fig. 5. The dispersion of the CO derived bands at an energy of roughly −7.0 eV (5σ and 1π) is very weak, only the CO-5σ orbital hybridizes and cannot always be clearly identified. The antibonding CO-$2\pi^*$ state is located at an energy of about 2 eV and distinctly visible between the $\bar{\Gamma}$ and $\bar{X}'$ point. In contrast to the Cu(110)-(2×1)O reconstruction, the adsorption of CO does not entirely destroy the characteristic surface states of the bare substrate. A Cu *s* like surface band can be found in the vicinity of the $\bar{Y}$ point with an onset energy of about 3 eV, 1.5 eV above the corresponding surface state of the bare surface.

Finally, we would like to point out a difference between DFT and experimental bands, leading to slightly shifted RDS features at higher energies. It was suggested that significant contributions to the Cu(110) RD signal are derived from bands between the bulk *L* and *W* points, which are anisotropically shifted in the vicinity of the surface. The respective

bands are projected onto the $\bar{S}$ point of the surface Brillouin zone in Fig. 4. Whereas experiments, based on the position of the involved bands, suggest an onset energy of 4.3 eV for the corresponding excitations, the DFT energy difference is slightly smaller (3.7 eV). As a general trend, the DFT band energies of all considered surfaces are shifted towards the Fermi energy compared to the experimental results.

C. Reflectance difference spectra of Cu(110), Cu(110)-(2×1)O, and Cu(110)-(2×1)CO

Calculations of the reflectance difference spectrum of the bare Cu(110) surface[14,15] and of the Cu(110)-(2×1)CO surface[16] have been performed by Monachesi *et al.* Their interpretation focused on the decomposition of single features of the RD spectra with respect to transitions between surface or bulklike states. We add the RD spectra of the Cu(110)-(2×1)O and Cu(110)-(3×1)CO surfaces and give a detailed interpretation of the RDS features with respect to the k point and energy origin of the contributing optical transitions. The differences between the spectra of Monachesi *et al.* and the RD spectra in this work arise from an increased number of slab layers used in the present approach (up to 25 layers instead of 11 layers). Also the previous linear muffin-tin orbital calculations (Refs. 14–16) were performed at the experimental constants and not the PBE lattice constants, which we have chosen in the present work. Other discrepancies are related to the different approaches concerning the treatment of the intraband transitions. In the present work, the plasma frequency was calculated *ab initio* and the relaxation time set to infinity, whereas Monachesi *et al.* used the experimental values and neglected anisotropies in the intraband plasma frequency tensor.

Figure 6 shows the theoretical reflectance difference spectra for the systems considered in the present work (left) and the corresponding experimental spectra[22] (right). The absolute values of the theoretical RD spectra are in good agreement with the experimental ones, especially for low frequencies. Most of the theoretical features are easily assigned to their experimental counterparts, although the theoretical features are generally shifted to lower energies. This is related to a shift of the theoretical band structure (both empty and filled states) towards the Fermi energy. Therefore, the DFT transition energies tend to be lower than in experiment, in particular, for higher frequencies.

The main RDS features of the bare surface, that is, the peak at an energy of about 2 eV and the two minima between 3 and 4.5 eV, are reproduced by the calculations. For the (2×1)O reconstruction, the calculations give a similar RD spectrum as the experiments in the low energy range and the minimum at higher energies is present, even though it is broader than in experiment, possibly an artifact of the finite slab size that could not be totally corrected by averaging over slabs with different thicknesses. If just the RD contributions from transitions in the region around the $\bar{Y}$ point are considered (dashed line in Fig. 6), which contain all main transitions characteristic of the (2×1)O reconstruction and involve excitations insensitive to the slab thickness, the correspondence with experiment is improved.

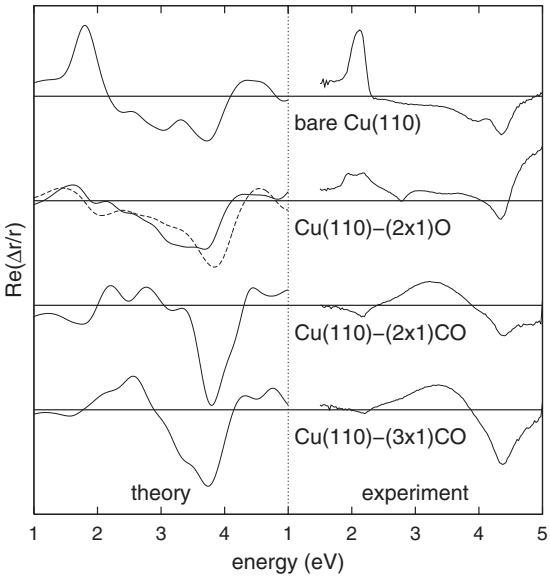

FIG. 6. RDS of the bare, of the oxygen, and of the carbon-monoxide-covered Cu(110) surface. The left panel shows the RD spectra calculated in this work, the right panel the experimentally measured spectra (Ref. 22). For the (2×1)O reconstruction, also the RD spectrum arising only from transitions in the vicinity of the $\bar{Y}$ point is shown using a dashed line.

In the case of the carbon-monoxide-covered surface, calculations correctly reproduce the change of the low energy RD from negative to positive, as well as the positive values around 3 eV. Furthermore, the agreement for the (3×1)CO surface is generally rather good even at high energies. The minimum around 4 eV is now very pronounced in the experiment and in the theoretical calculations. The results for the (2×1)CO surface are somewhat disappointing in the high energy regime (>3 eV). In the density functional theory calculations, the minimum around 4 eV has become even more pronounced, whereas the opposite is observed in experiment. We, however, note that Hofmann *et al.*[18] also observed a rather deep minimum at 1/2 monolayer (ML) CO coverage. Preparation of the surface at 1/2 ML CO coverage is not straightforward, and differences in the degree of ordering can affect the experimental spectrum. However, it is also possible that states related to CO are less reliably predicted using present density functionals, a point that we will return to in Sec. IV.

The optical anisotropy of the bare Cu(110) surface mainly arises from transitions in the vicinity of the $\bar{Y}$ and $\bar{S}$ points of the (1×1) surface Brillouin zone. At the $\bar{Y}$ point, transitions from the occupied surface band at −0.5 eV to the unoccupied surface band at 1.5 eV lead to a small reflectance (or high absorption) of light polarized along the y direction at an energy of about 2 eV. This confirms former assumptions concerning the origin of this pronounced maximum for the bare surface[18,20,25] and also agrees with the results of Monachesi *et al.*[14,15] The final shape of the 2 eV peak is given by the interplay between transitions at the $\bar{X}$ point from d_{xy}-like bands at the top of the d bands to the p_x bands at the Fermi energy (positive RDS contribution) and respective transitions

to the p_y-like bands between the $\bar{\Gamma}$ and $\bar{Y}$ points (negative RDS contribution), resulting in a small positive RDS shoulder at about 2 eV. This kind of contribution to the RDS feature around 2 eV was proposed by Sun *et al.*[25]

The pronounced RDS minimum at about 3.8 eV relates to transitions from p_x- and p_y-like bands at the Fermi energy to the unoccupied s bands at the $\bar{S}$ point. States with both characters (p_x and p_y) can be found at the Fermi energy close to the $\bar{S}$ k point nevertheless, the surface contribution of p_x-like orbitals is significantly stronger due to the anisotropy of the surface. This is mirrored by the dielectric function, which shows contributions for light polarized in both the x and y directions, but with a preference by about a factor of 2 for absorption of x-polarized light. Although the very same bands were associated with the respective RDS minimum by Sun *et al.*,[21] theory cannot explicitly relate this minimum to a small energy shift of the x and y dielectric functions with respect to each other. The bands assigned to the minimum at 3.8 eV are not sensitive to adsorption: therefore, the feature remains present for both the (2×1)O and (2×1)CO surfaces. At slightly lower energies, the RD spectrum of the bare Cu(110) surface exhibits another minimum at 3 eV, arising from transitions in the vicinity of the $\bar{Y}$ point. It is related to transitions from a d_{xz} surface resonance at the top of the d bands to the unoccupied surface band at 1.5 eV. The transition probability for such an excitation is nonzero because the unoccupied band has some p_z character.

We now focus on the (2×1)O and (2×1)CO surfaces. Because the surface cell of these phases is two times larger than for the bare surface, the respective Brillouin zone is folded back in the x direction, e.g., the $\bar{\Gamma}$ point region now contains $\bar{\Gamma}$ and $\bar{X}$ contributions from the (1×1) surface Brillouin zone, and the $\bar{Y}$ point contributions from both the (1×1) $\bar{Y}$ and $\bar{S}$ points. In the following discussion, we will use the (2×1) notation, if not otherwise stated.

Although the RD spectra for the (2×1)O and (2×1)CO structures look very different at first glance, an analysis with respect to contributions from different k-point regions shows that the main difference only arises from the Brillouin zone edge between the $\bar{Y}$ and $\bar{S}'$ points.

For lower energies, the RD spectrum of the (2×1)CO surface can be taken as the starting point for the interpretation of both (2×1) spectra. The negative RD signal at energies lower than 2 eV is not easily assigned to specific transitions. It is rather the effect of a general shift between the x and y dielectric functions. For low energies, the dielectric function of the (2×1)CO surface resembles the bulk one, but the dielectric function in the x direction sets in at a slightly lower energy (about 0.08 eV earlier than the one in the y direction). Hence the low energy part of the (2×1)CO RD spectrum can be described by a derivative model.[45]

For the (2×1)O surface, this negative signal at low energies is compensated by RD contributions from transitions between and to surface states at the $\bar{Y}$ point associated with the adsorbed oxygen. The form of the RD spectrum in the low energy region, the hump at 1.5 eV, and the following minimum at 2.1 eV can be divided into three different parts. The first part can be assigned to transitions from O p_z states at −1.0 eV to O p_y states at 0.5 eV. The second is due to transitions from bulklike states with p_y character at energies between −1.5 and −1.0 eV to the unoccupied O p_y state. Both lead to a positive RD signal with a RD maximum at 1.5 eV. The third part, resulting in the minimum at 2 eV, has its origin in excitations from bulklike d bands slightly below the upper d band edge to the very same O p_y state. A detailed analysis shows that d bands with significant d_{xz} character are involved in these transitions.

The RD spectra for energies higher than 3 eV are dominated by the minimum at 3.8 eV for both the (2×1)O and (2×1)CO surfaces as discussed above. In contrast to experiment, this minimum is larger for the (2×1)CO surface than for the bare and (2×1)O surfaces. An analysis of the imaginary part of the dielectric function of the (2×1)CO surface in x and y directions reveals a small, almost Gaussian-like absorption peak at about 3.4 eV for light polarized along the y direction. The matching excitations are from Cu p_y bulklike states to the (2×1)CO surface state at about 3 eV. At energies of about 3 eV, the value of the imaginary part of the bulk dielectric function exceeds that of the real part, so that the influence of the real part of the surface dielectric functions becomes crucial. For the transitions discussed here, this yields a negative peak in the RD spectrum at an energy of about 3.7 eV, enhancing the already existing one.

In order to clarify the reason for the different amplitudes of the minimum given by experiment and theory, we additionally calculated the reflectance difference spectrum for the (3×1)CO surface. Here, we also found an enlarged minimum compared to the bare Cu(110) surface, related to an unoccupied Cu s surface state with a lower onset than that of the (2×1)CO surface. The depth of the minimum now is in agreement with the experimental data (see Ref. 22 and Fig. 6). Experiment shows that the intensity, the position, and the line shape of the RDS features at 4 eV are quite sensitive to surface defects, the roughness of the surface, and the presence or absence of adsorbate induced surface stresses. If the influence of these factors is neglected (surface defects and surface roughness), the experimental and theoretical RD spectra will show deviations at 4 eV.

IV. DISCUSSION AND CONCLUSIONS

We performed *ab initio* density functional theory calculations of the optical properties of the bare Cu(110), the oxygen reconstructed Cu(110)-(2×1)O, and the carbon-monoxide covered Cu(110)-$(n\times1)$CO ($n=2,3$) surfaces. All these surfaces are anisotropic and, therefore, respond differently to incident light polarized in two orthogonal directions, resulting in a nonvanishing reflectance difference (RD) signal.

The optical properties of these surfaces, represented by slabs with up to 25 layers, were calculated within the independent particle picture. The two simplifications applied in the present work, namely, the use of DFT one-electron energies and wave functions as input for the calculation of the surface and bulk dielectric functions and the mapping of the

macroscopic surface onto a finite slab, have to be handled carefully. Concerning the finite size of the model surface, we found that optical features related to transitions between surface states converge fast with the number of layers, but transitions related to bulklike states filling up the continuum introduce spurious oscillations. Furthermore, we found it essential to calculate the surface intraband plasma frequency tensor exactly and consistently with the interband contributions in order to remedy the large thickness-dependent interband anisotropy introduced by bands crossing at the Fermi edge.

When discussing the validity of the DFT approach as a basis for the calculation of optical spectra, we have to note that there is no formal reason why quasiparticle energies should or could be related to the one-electron energies predicted by density functional theory, even if the exact adiabatic density functional was known. Only time-dependent density functional theory would allow to do so, but presently no universal time-dependent functional is available. If we refer in the following to density functional errors, we always mean errors related to the time-independent density functionals used here.

The comparison of the three calculated RD spectra with the experimental ones demonstrates that an *ab initio* treatment, as used in this work, is able to reproduce the main features of the experimental spectra. In particular, at energies below 2.5 eV, the behavior is correctly reproduced. For the bare Cu(110) surface, a strong resonance is observed, which is progressively reduced from the bare surface, over the Cu(110)-(2×1)O surface, to the Cu(110)-$(n\times1)$CO surface, where the experimental and theoretical RD spectra even show a shallow minimum at around 1.5 eV. Generally, the theoretical spectra are redshifted compared to experiment, which can be related to approximately 15% too small transition energies predicted by the present gradient corrected density functionals. The underestimation of band gaps and excitation energies is a well known deficiency of DFT, which obviously prevails for metallic surfaces such as the Cu(110) surface. At higher energies, we observe that the agreement with experiment becomes progressively worse. Reasonable results at energies beyond 2.5 eV are obtained for the bare Cu(110) surface, which shows, in agreement with experiment, two minima, with the second one being related to the transition from states at the Fermi level to *s*-like bands at the $\bar{S}$ *k* point. Again the transition energies are underestimated by $\approx$15%. For the Cu(110)-(2×1)O surface, the theoretical minimum deepens and blueshifts slightly. Experiment also shows a blueshift but, at the same time, a reduction of the minimum is observed. The reason for this discrepancy is most likely related to the present density functionals. For the bare surface, the errors introduced by the applied density functional generally result in a 10%–20% shift of all transitions to lower energies. Once a second species, in this case, O, is introduced, the errors for Cu and O related states are likely to be different due to the different degrees of localization of these states.

It is not astonishing that this trend prevails and becomes even worse for the CO covered surfaces. It is very likely that the applied density functionals will show more substantial errors for the localized CO orbitals than for the delocalized surface states. We recall that all available density functionals result in substantial self-interaction errors, shifting occupied states too strongly toward the Fermi level, concomitantly strongly reducing excitation energies. Errors in transition energies related to localized CO states might well exceed 20%. Since RDS is a method that depends strongly on the relative position of states, different shifts for different states can destroy agreement with experiment. This is exactly what we believe to happen at higher energies, where states with O-like character for the Cu(110)-(2×1)O, and CO-like character for the Cu(110)-(2×1)CO surface become important. It is, thus, likely that errors are related to the fact that adsorbate induced states do not show the same uniform shift as metal states.

We conclude that density functional theory is a reasonable but far from perfect starting point for the calculation of optical spectra of metallic surfaces. For the bare substrate, agreement is good, but it becomes progressively worse for adsorbate covered surfaces, in particular, for those with localized states introduced by adsorbates.

ACKNOWLEDGMENT

This work was supported by the Austrian *Fonds zur Förderung der Wissenschaftlichen Forschung* (FWF) under Contract No. S9002, No. S9008, and No. Y218.

*georg.kresse@univie.ac.at

[1] P. Weightman, D. S. Martin, R. J. Cole, and T. Farrell, Rep. Prog. Phys. **68**, 1251 (2005).

[2] D. S. Martin and P. Weightman, Surf. Interface Anal. **31**, 915 (2001).

[3] J. D. E. McIntyre and D. E. Aspnes, Surf. Sci. **24**, 417 (1971).

[4] D. E. Aspnes, J. Vac. Sci. Technol. B **3**, 1138 (1985).

[5] D. E. Aspnes, J. P. Harbison, A. A. Studna, and L. T. Florez, J. Vac. Sci. Technol. A **6**, 1327 (1988).

[6] N. Wiser, Phys. Rev. **129**, 62 (1963).

[7] S. L. Adler, Phys. Rev. **126**, 413 (1962).

[8] E. G. Maksimov, I. I. Mazin, S. N. Rashkeev, and Y. A. Uspenski, J. Phys. F: Met. Phys. **18**, 833 (1988).

[9] K.-H. Lee and K. J. Chang, Phys. Rev. B **49**, 2362 (1994).

[10] I. Campillo, A. Rubio, and J. M. Pitarke, Phys. Rev. B **59**, 12188 (1999).

[11] H. Ebert, Rep. Prog. Phys. **59**, 1665 (1996).

[12] V. N. Antonov, A. N. Yaresko, A. Ya. Perlov, V. V. Nemoshkalenko, P. M. Oppeneer, and H. Eschrig, Low Temp. Phys. **25**, 387 (1999).

[13] J. Kuneš and P. Novák, J. Phys.: Condens. Matter **11**, 6301 (1999).

[14] P. Monachesi, M. Palummo, R. Del Sole, R. Ahuja, and O. Eriksson, Phys. Rev. B **64**, 115421 (2001).
[15] P. Monachesi, M. Palummo, R. Del Sole, A. Grechnev, and O. Eriksson, Phys. Rev. B **68**, 035426 (2003).
[16] P. Monachesi and L. Chiodo, Phys. Rev. Lett. **93**, 116102 (2004).
[17] Th. Herrmann, M. Gensch, M. J. G. Lee, A. I. Shkrebtii, N. Esser, W. Richter, and Ph. Hofmann, Phys. Rev. B **69**, 165406 (2004).
[18] Ph. Hofmann, K. C. Rose, V. Fernandez, A. M. Bradshaw, and W. Richter, Phys. Rev. Lett. **75**, 2039 (1995).
[19] U. Rossow, L. Mantese, and D. E. Aspnes, Appl. Surf. Sci. **123/124**, 237 (1998).
[20] K. Stahrenberg, Th. Herrmann, N. Esser, and W. Richter, Phys. Rev. B **61**, 3043 (2000).
[21] L. D. Sun, M. Hohage, P. Zeppenfeld, R. E. Balderas-Navarro, and K. Hingerl, Surf. Sci. **527**, L184 (2003).
[22] L. D. Sun, M. Hohage, P. Zeppenfeld, and R. E. Balderas-Navarro, Phys. Status Solidi C **0**, 3022 (2003).
[23] L. D. Sun, M. Hohage, P. Zeppenfeld, R. E. Balderas-Navarro, and K. Hingerl, Phys. Rev. Lett. **90**, 106104 (2003).
[24] L. D. Sun, M. Hohage, and P. Zeppenfeld, Phys. Rev. B **69**, 045407 (2004).
[25] L. D. Sun, M. Hohage, P. Zeppenfeld, and R. E. Balderas-Navarro, Surf. Sci. **589**, 153 (2005).
[26] M. Gajdoš, K. Hummer, G. Kresse, J. Furthmüller, and F. Bechstedt, Phys. Rev. B **73**, 045112 (2006).
[27] P. Ziesche and G. Lehmann, *Elektronentheorie der Metalle* (Springer-Verlag, Berlin, 1983).
[28] G. Kresse and J. Hafner, Phys. Rev. B **48**, 13115 (1993).
[29] G. Kresse and J. Furthmüller, Comput. Mater. Sci. **6**, 15 (1996).
[30] P. E. Blöchl, Phys. Rev. B **50**, 17953 (1994).
[31] G. Kresse and D. Joubert, Phys. Rev. B **59**, 1758 (1998).
[32] J. P. Perdew, K. Burke, and M. Ernzerhof, Phys. Rev. Lett. **77**, 3865 (1996).
[33] S. Y. Liem, G. Kresse, and J. H. R. Clarke, Surf. Sci. **415**, 194 (1998).
[34] J. Harl and G. Kresse, Surf. Sci. **600**, 4633 (2006).
[35] Ph. Hofmann, K.-M. Schindler, S. Bao, V. Fritzsche, A. M. Bradshaw, and D. P. Woodruff, Surf. Sci. **337**, 169 (1995).
[36] M. Methfessel and A. T. Paxton, Phys. Rev. B **40**, 3616 (1989).
[37] D. Brust, Phys. Rev. B **2**, 818 (1970).
[38] F. Szmulowicz and B. Segall, Phys. Rev. B **24**, 892 (1981).
[39] P. B. Johnson and R. W. Christy, Phys. Rev. B **6**, 4370 (1972).
[40] A. Marini, G. Onida, and R. Del Sole, Phys. Rev. Lett. **88**, 016403 (2002).
[41] S. Kevan, Phys. Rev. B **28**, 4822 (1983).
[42] A. Goldmann, V. Dose, and G. Borstel, Phys. Rev. B **32**, 1971 (1985).
[43] *Solid State Physics*, edited by G. Chiarotti, Landolt-Börnstein, New Series, Group III, Vol. 24, Pt. B (Springer, Berlin, 1995).
[44] R. Courths, S. Hüfner, P. Kemkes, and G. Wiesen, Surf. Sci. **376**, 43 (1997).
[45] U. Rossow, L. Mantese, and D. E. Aspnes, J. Vac. Sci. Technol. B **14**, 3070 (1996).